The EMBO Journal (2011) 30, 2705–2718 | © 2011 European Molecular Biology Organization | All Rights Reserved 0261-4189/11
www.embojournal.org

THE EMBO JOURNAL

A hypomorphic IgH-chain allele affects development of B-cell subsets and favours receptor editing

Sven Brenner[1], Diana Drewel[1], Thomas Steinbart[1], Florian Weisel[1], Eric Härtel[1], Sonja Pötzsch[1], Heike Welzel[1], Andreas Brandl[2], Philipp Yu[3], Geert C Mudde[4], Astrid Schweizer[5], Lars Nitschke[5] and Thomas H Winkler[1,*]

[1]Department of Biology, Nikolaus-Fiebiger-Center for Molecular Medicine, Friedrich-Alexander-University Erlangen-Nuremberg, Erlangen, Germany; [2]Division of Molecular Immunology, Department of Internal Medicine III, Nikolaus-Fiebiger-Center for Molecular Medicine, Friedrich-Alexander-University Erlangen-Nuremberg, Erlangen, Germany; [3]Institute for Immunology, Philipps-University Marburg, Marburg, Germany; [4]S-TARget Therapeutics, Vienna, Austria and [5]Department of Biology, Friedrich-Alexander-University Erlangen-Nuremberg, Erlangen, Germany

The quality and quantity of BCR signals impact on cell fate decisions of B lymphocytes. Here, we describe novel gene-targeted mice, which in the context of normal VDJ recombination show hypomorphic expression of immunoglobulin μ heavy chain (μHC) mRNA levels and hence lower pre-BCR and BCR levels. Hypomorphic expression of μHC leads to augmented selection processes at all stages of B-cell development, noticeably at the expansion of pre-B cells, the positive selection of immature B lymphocytes in the bone marrow and the selection of the follicular (FO), marginal zone (MZ) and B1 B-lymphocyte compartment in peripheral lymphoid organs. Immature as well as mature FO and MZ B lymphocytes in the peripheral lymphoid organs express lower levels of the receptor for B-cell activating factor (BAFF). In addition, hypomorphic expression of the BCR favours receptor editing. Together, our results highlight the critical importance of pre-BCR and BCR receptor levels for the normal development of B-lymphocyte subpopulations in the context of intact VDJ recombination and a diverse antibody repertoire.

The EMBO Journal (2011) **30,** 2705–2718. doi:10.1038/emboj.2011.168; Published online 27 May 2011
Subject Categories: Immunology
Keywords: BAFF; B-cell development; B-cell receptor; receptor editing

*Corresponding author. Department of Biology, Friedrich-Alexander-University Erlangen-Nuremberg, Nikolaus-Fiebiger-Center for Molecular Medicine, Glueckstrasse 6, 91054 Erlangen, Germany. Tel.: +49 9131/85 29136; Fax: +49 9131/85 29106; E-mail: twinkler@molmed.uni-erlangen.de

Received: 23 November 2010; accepted: 4 May 2011; published online: 27 May 2011

Introduction

B-cell development in fetal liver and adult bone marrow (BM) occurs in several consecutive steps. Successful assembly of an immunoglobulin μ heavy chain (μHC) with the surrogate light chain (SLC) to a complex known as pre-BCR allows cells to pass the first developmental checkpoint. Subsequent proliferation of large pre-B cells ensures the selective expansion of precursors expressing a functional μHC (Hess *et al*, 2001). Upon cell-cycle exit, large pre-B cells differentiate into resting small pre-B cells in order to rearrange V and J gene segments on their immunoglobulin light chain (LC) loci. Functional LCs pair with μHCs and are then expressed as BCR on the surface of the immature B cell. Not all cells directly proceed in the developmental program, however. Those with a BCR reactive to self-antigen are clonally deleted, achieve anergy or are rescued by receptor editing. By the latter process, cells eliminate their initial BCR specificity and replace it by a product of secondary LC rearrangements possibly resulting in an innocuous BCR (Gay *et al*, 1993; Tiegs *et al*, 1993). BCRs that have insufficient capacities to be expressed on the cell surface are also thought to be removed from the mature repertoire since they are not able to effectively downregulate expression of RAG and hence force ongoing somatic recombination (Nemazee and Hogquist, 2003).

The majority of immature BM-derived B cells expressing appropriate BCRs mature in the spleen (Allman and Pillai, 2008) differentiating into either follicular (FO) or marginal zone (MZ) B cells. FO B cells are recirculating cells and thus migrate through blood and lymph vessels to the BM and B-cell areas of lymph nodes, Peyer's patches and spleen. Their main functional role is to mediate T-dependent immune responses to protein antigens. In contrast, MZ B cells represent a self-renewing population (Hao and Rajewsky, 2001; and reviewed in Martin and Kearney (2002)) mainly positioned between the marginal sinus and the red pulp of the spleen. The peritoneal and pleural cavities of mice are primarily inhabited by a population of self-replenishing B lymphocytes derived from fetal precursors (Dorshkind and Montecino-Rodriguez, 2007). They are termed B1 cells in contrast to both BM-derived MZ B and FO B cells, which are also referred to as B2 cells. The B1 subset is further classified into B1a and B1b cells with respect to differential expression of the surface marker CD5 (Kantor and Herzenberg, 1993). $CD5^+$ B1a cells spontaneously secrete natural IgM and thus provide a first line of defense against T-independent antigens, for example, encapsulated bacteria (Haas *et al*, 2005). $CD5^-$ B1b cells lack this competence but upon induced antibody secretion they help clearing the pathogen and provide long-term protection (Alugupalli *et al*, 2004).

In the past two decades, a large number of studies most notably by using gene-targeted mice contributed to unravel various mechanisms of B-cell development. However, it is

still a matter of debate to what extent BCR signalling strength is involved in cell fate decisions. According to a 'signalling-strength-model' weak, intermediate and strong BCR signals are linked to the development of MZ B, FO B and B1 lymphocytes, respectively. For instance lack of negative regulators of BCR signalling such as SHP-1, SiglecG or Lyn lead to increased B1-cell numbers. Concordantly, deletion of positive regulators like Btk, PLCγ2 or SLP65 results in a decreased B1:B2 ratio (for detailed review, see Berland and Wortis, 2002).

In this report, we describe a novel mouse model that carries a targeted integration of a GFP gene located between the μ intronic enhancer (Eμ) and the constant region of the μHC locus. Contrary to our expectations, homozygous mutants are able to express functional BCRs. However, μHC mRNA levels are only a fraction of those found in wild-type (WT) controls leading to reduced receptor density and thus to diminished receptor signals. Since hypomorphic μHC expression offers a well-suited model for the investigation of attenuated receptor signalling, we analysed the impact of this mutation on B-cell development and on the emergence of peripheral B-cell subsets.

Results

Generation of IgH$^{Eμ\text{-}GFP/Eμ\text{-}GFP}$ mice

The μHC locus carries the intronic enhancer element Eμ between the last J gene (J_H4) of the variable region and the first exon of the constant region (Cμ1). We applied gene-targeting techniques to replace parts of the sterile transcript, which starts within the enhancer sequence (Lennon and Perry, 1985), by a gfp reporter gene. To monitor sterile transcripts initiating from Eμ, the gfp reporter gene was integrated in the μHC^a allele of a 129/Sv-derived ES cell line immediately downstream of Eμ without deleting any enhancer sequences (Supplementary Figure S1A). As we intended to measure dynamic changes of enhancer activity, we used a gfp gene encoding a destabilized protein. Correct integration of the targeting construct was detected by Southern blot analysis (Supplementary Figure S1B) and deletion of the neomycin resistance marker was mediated by protamine-cre (encoded in the ES cell genome) gaining function during spermatogenesis of chimeras (O'Gorman *et al*, 1997).

Targeted mice were backcrossed to the C57BL/6 strain. μHC alleles in C57BL/6 mice are of the b-allotype thus enabling us to clearly distinguish homozygous (IgH$^{Eμ\text{-}GFP/Eμ\text{-}GFP}$) and heterozygous (IgH$^{Eμ\text{-}GFP/b}$) animals from WT controls (IgH$^{b/b}$) even in flow cytometry by means of their differential expression of the IgM allotypes a and b (IgM^a and IgM^b).

B cells from homozygous IgH$^{Eμ\text{-}GFP}$ mice express reduced μHC mRNA levels

Flow cytometric analyses of heterozygous and homozygous knock-in mice revealed only very poor GFP expression levels at any stage of B-cell development (Supplementary Figure S1C). This is probably due to rapid degradation of the destabilized GFP protein. In contrast to our initial expectations, B-cell development in homozygous IgH$^{Eμ\text{-}GFP/Eμ\text{-}GFP}$ mice was not arrested at the pro-B-cell stage (Figure 1). The most probable reason for the development of Ig$^+$ B cells despite the strong polyadenylation (pA) site within the Eμ region is that the pA site is skipped to a certain extent, resulting in the generation of a regular μHC mRNA in a certain number of transcription events (Supplementary Figure S2). To address this hypothesis, we performed QPCR analyses to measure μHC mRNA levels in sorted cell populations from IgH$^{Eμ\text{-}GFP/Eμ\text{-}GFP}$ mice and WT mice (Table I). Indeed, B-cell populations from homozygous mutants displayed a clear reduction of specific μHC mRNA levels compared with those from WT controls as measured for pre-B, MZ B and FO B cells. This effect was more pronounced when forward primers annealing within the J_H4 segment as compared with the J_H2 segment were used, indicating that the shorter distance between the J_H4 segment and the artificial pA site favours polyadenylation versus splicing. We conclude that the insertion of the gfp-pA cassette 3′ of Eμ created a hypomorphic mutation of the IgH locus with a 2- to 10-fold reduction of μHC mRNA levels, depending on the J_H usage and the stage of development of B lymphocytes.

BM B-cell development is partially blocked in IgH$^{Eμ\text{-}GFP/Eμ\text{-}GFP}$ mice

To determine whether hypomorphic μHC expression had an impact on the development of B cells, we analysed the distribution of distinct B-cell subsets in the BM by FACS. B220 and CD19 staining revealed that total numbers of

Table I Reduced μHC mRNA levels in sorted B-cell subsets from IgH$^{Eμ-GFP/Eμ-GFP}$ mice

PCR primers	Cell subset		
	Pre-B cells	MZ B cells	FO B cells
JH_2–Cμ$_1$	19 ± 7[a]	45 ± 12	70 ± 10
JH_4–Cμ$_1$	9 ± 4	9 ± 6	15 ± 8

[a]μHC mRNA levels in B-cell subsets from IgH$^{Eμ-GFP/Eμ-GFP}$ mice are presented as percentage of WT levels (mean ± s.d.). Data are based on 2–3 independent cell sorts followed by QPCR analysis. Cells from individual mice or pooled cells from 2 to 3 mice of each genotype were used for cell sorting. Two different JH_4 primers were used.

Figure 1 B-cell development in BM of IgH$^{Eμ\text{-}GFP/Eμ\text{-}GFP}$ mice is partially blocked. (**A**) Flow cytometric analysis of B lineage-specific surface markers in the BM of WT mice (IgH$^{b/b}$), heterozygous mutant mice (IgH$^{Eμ\text{-}GFP/b}$) and homozygous mutant mice (IgH$^{Eμ\text{-}GFP/Eμ\text{-}GFP)}$. Expression profiles of the indicated markers are illustrated as density plots. Numbers above or adjacent to gates indicate percentages of B-cell subsets: total B-lymphoid cells (B220$^+$/CD19$^+$), pro-B cells (B220$^+$/ckit$^+$), pre-B cells (B220$^+$/CD25$^+$), recirculating B cells (B220^{high}/ckit$^-$ or B220^{high}/CD25$^-$), immature B cells (B220^{low}/IgM^{int}), transitional B cells (B220^{int}/IgM^{high}) and mature B cells (B220^{high}/IgM^{int}). Data are representative of six independent experiments with similar results. (**B**) Total numbers of B cells (B220$^+$/CD19$^+$) and relative numbers of pro-B, pre-B, immature B and mature B cells within the CD19$^+$ gate. Bars represent mean values and the s.e.m. of six animals for each genotype. $^*P<0.05$; $^{***}P<0.001$ (Mann-Whitney test). (**C**) FACS of cytoplasmic μHC expression in pre-B cells of indicated mice is shown as histogram overlay. μHC expression in B220$^-$/CD25$^-$ cells from WT mice is included in the overlay as an internal negative control. The orange arrow points to the presumed μHC^a-expressing pre-B cells in heterozygous mice. (**D**) Flow cytometric analysis of CD19 and IgM^a expression in splenic lymphocytes from heterozygous mice. WT mice and BDF1 mice served as negative and positive controls for IgM^a expression, respectively. Relative percentages of cells are given in each quadrant. Data are representative of four independent experiments with similar results.

B cells among BM lymphocyte populations were reduced in $IgH^{E\mu\text{-}GFP/E\mu\text{-}GFP}$ mice whereas B-cell numbers in heterozygous animals ($IgH^{E\mu\text{-}GFP/b}$) were in between those of WT mice and homozygous mutants (Figure 1A and B). Homozygous mutants had a higher frequency of $ckit^+$ pro-B cells (Figure 1B). In addition, the frequency of immature B cells

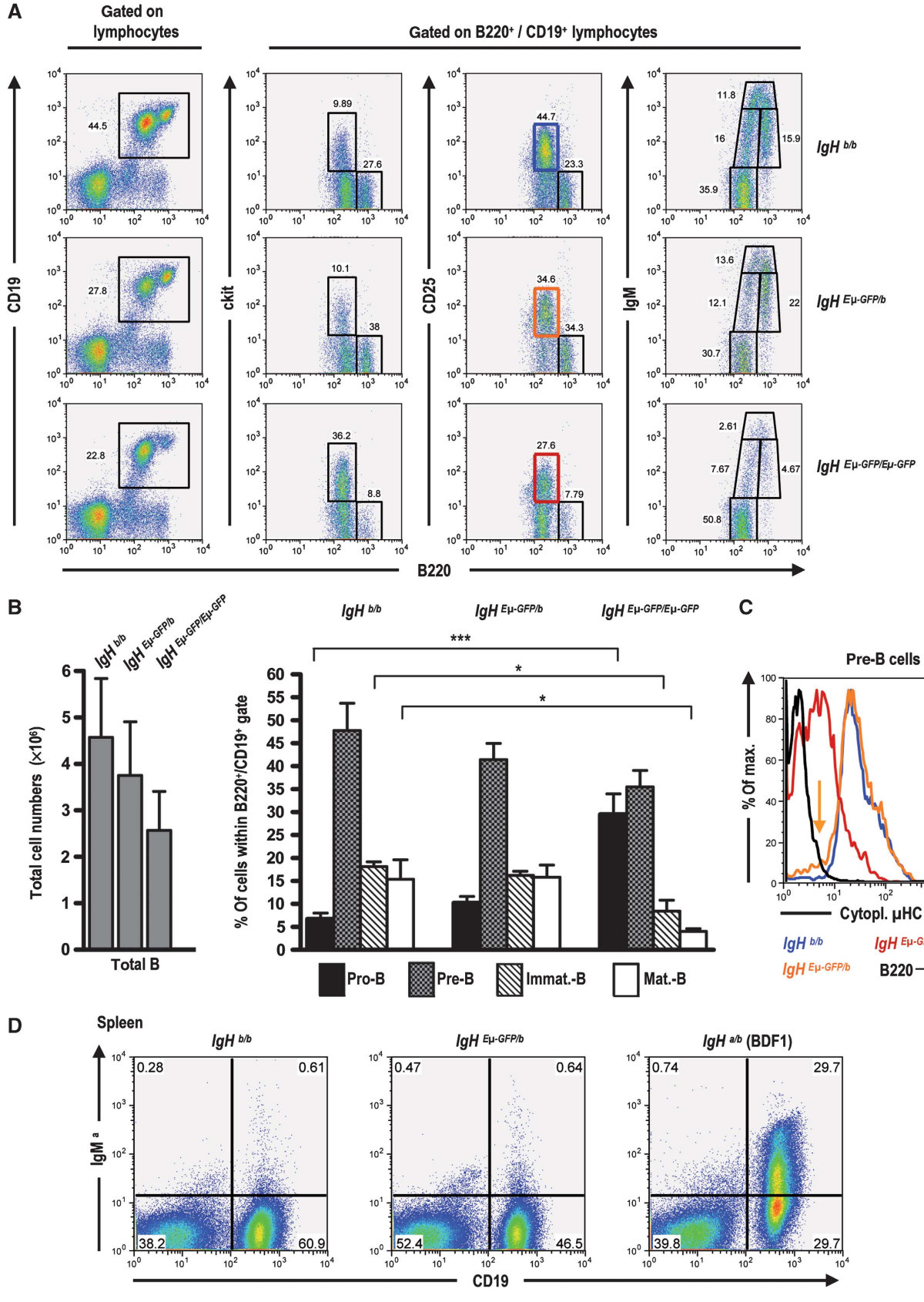

was reduced in $IgH^{E\mu\text{-}GFP/E\mu\text{-}GFP}$ mice, resulting in a higher ratio of pre-B to immature B cells (Figure 1A and B). Finally, we observed an immature B to mature B-cell ratio of about 2:1 in homozygous mutant mice being clearly higher as in WT controls, which displayed a ratio of 1:1, suggesting that also immature B cells of homozygous mutants are impaired in their further maturation process. We conclude that hypomorphic μHC expression leads to a partial block of B-cell development at the pro-B to pre-B, the pre-B to immature B as well as the immature B to mature B-cell stages of development.

Distribution of developmental B-cell subsets in heterozygous mice was more similar to WT mice than to homozygous mice. However, the pro-B-cell compartment was clearly enlarged in heterozygous animals whereas pre-B cells were slightly reduced (Figure 1A and B).

Since B-cell development in homozygous $IgH^{E\mu\text{-}GFP/E\mu\text{-}GFP}$ mice was impaired at designated stages, we wanted to figure out to what extent hypomorphic μHC^a-expressing lymphocytes in heterozygous animals were able to 'compete' with μHC^b-expressing cells that express normal μHC levels. As there is no allotype-specific antibody available, which reacts either with free μHC or with μHC complexed with the SLC in B-cell precursors, it was impossible to distinguish between μHC^a- and μHC^b-positive cells before the immature B-cell stage in heterozygous mice by FACS analysis. As expected from the QPCR data, pre-B cells from $IgH^{E\mu\text{-}GFP/E\mu\text{-}GFP}$ mice contained ~5- to 10-fold lower levels of cytoplasmic μHC protein when compared with WT pre-B cells (Figure 1C). In heterozygous mice, the majority of pre-B cells showed WT levels of cytoplasmic μHC protein, presumably from the WT μHC^b allele. Only a very small, but reproducible fraction of pre-B cells expressed low μHC levels comparable to μHC levels in homozygous mutants (indicated by the orange arrow in Figure 1C), most likely representing μHCs from the mutant μHC^a allele. These results suggested that in heterozygous mice only a small fraction of μHC^a-expressing precursors reached the pre-B-cell stage. To assess whether any B cells with hypomorphic μHC^a expression were actually capable of taking part in the mature repertoire of heterozygous mice, we stained for surface-IgM^a on splenocytes from these animals (Figure 1D). Indeed, IgM^a-expressing cells were below detection limits when comparing $IgH^{E\mu\text{-}GFP/b}$ mice with their WT littermates lacking the μHC^a allele.

As B-cell development was strongly impaired in $IgH^{E\mu\text{-}GFP/E\mu\text{-}GFP}$ mice and IgM^a-expressing B cells were not detectable in the periphery of heterozygous mice, we next wanted to exclude the possibility that VDJ recombination on the mutant μHC^a allele was impaired by the targeted integration of the gfp-cassette. To this end, we tested for the relative amount of non-productive somatic VDJ rearrangements of the μHC^a allele in sorted IgM^b-expressing splenic B cells from heterozygous mutant mice and from WT (C57Bl/6xDBA/2) F1 mice (BDF1 mice, $IgH^{a/b}$). Non-productive recombination events would be reduced in B cells from heterozygous mutant mice if VDJ recombination was impaired by the targeted insertion of the gfp-cassette. By analysing non-productive recombination events, any selection at the pre-B or immature B-cell stage is avoided. VDJ_H1, VDJ_H2 and VDJ_H3 recombinations were amplified and the PCR products were digested with the restriction enzyme *Afl*II, which digests μHC^a but not μHC^b alleles between JH_3 and JH_4 segments (Supplementary Figure S3A). Somatic VDJ rearrangements of the mutant μHC^a allele in IgM^{b+} B cells from heterozygous mutant mice and the WT μHC^a allele in BDF1 controls were observed in similar ratios as compared with the μHC^b alleles for V_H segments of both the 7183 as well as the J558 V_H family (Supplementary Figure S3B), suggesting a largely normal VDJ recombination at the targeted μHC allele. In summary, the partial developmental blocks at several B-cell developmental stages in the BM of $IgH^{E\mu\text{-}GFP/E\mu\text{-}GFP}$ mice resulted from reduced μHC expression.

Enforced receptor editing in $IgH^{E\mu\text{-}GFP/E\mu\text{-}GFP}$ mice

It has been proposed that a certain threshold level of constitutive (tonic) antigen receptor signalling is necessary for positive selection of immature B cells and downregulation of RAG expression (Nemazee and Hogquist, 2003; Tze *et al*, 2005). Since homozygous mutants comprised a repertoire of B cells that was altogether characterized by a reduction of μHC expression these mice are well suited to confirm this hypothesis. As shown in Figure 1B, differentiation from pre-B to immature B lymphocytes was noticeably impaired in $IgH^{E\mu\text{-}GFP/E\mu\text{-}GFP}$ mice, suggesting impairment in positive selection in these animals. To test for receptor editing, we first determined relative numbers of κ-LC- and λ-LC-expressing cells in the BM as well as in the periphery of $IgH^{E\mu\text{-}GFP/E\mu\text{-}GFP}$ and WT mice by FACS (Figure 2A and B). The ratios of κ-LC- to λ-LC-expressing cells in the BM of homozygous mutant mice were significantly lower as compared with WT controls (4.4:1 versus 13.1:1, Figure 2B). Also in the spleen and the peritoneal cavity (PC) of $IgH^{E\mu\text{-}GFP/E\mu\text{-}GFP}$ mice, the ratios of κ-LC- to λ-LC-expressing cells were significantly lower (8.1:1 to 27.0:1 for spleen and 7.6:1 to 19.9:1 for PC). Enforced receptor editing not only result in higher frequencies of λ-LC-expressing B cells but also in increased usage of distal Jκ gene segments (Radic *et al*, 1993; Tiegs *et al*, 1993). To verify if $IgH^{E\mu\text{-}GFP/E\mu\text{-}GFP}$ mice exhibited an altered Jκ usage, we used cDNA from $CD19^+$ splenocytes as template for the amplification of VκJκCκ fragments. Subsequently, these LC segments were cloned and sequenced to determine the Jκ usage (Figure 2C). As expected, B cells from a WT mouse preferentially used the proximal Jκ1 element. In contrast, the downstream Jκ5 was predominantly used in splenic B cells from an $IgH^{E\mu\text{-}GFP/E\mu\text{-}GFP}$ mouse. Interestingly, we did not observe an altered usage of Jκ2 and Jκ4 segments. Together, these findings are clear evidence of enforced receptor editing in the homozygous mutants, as a consequence of decreased μHC expression at the stage of immature B cells.

To test, whether B cells have a failure to shut off Rag gene expression at the immature B-cell stage, we performed QPCR analyses for Rag-2 expression from sorted immature cell populations. As shown in Supplementary Figure S4, immature B cells from mutant mice showed slightly less Rag-2 transcript levels than WT immature B cells.

Altered distribution of splenic B-cell subsets in $IgH^{E\mu\text{-}GFP/E\mu\text{-}GFP}$ mice

As described above, B-cell development in the BM of $IgH^{E\mu\text{-}GFP/E\mu\text{-}GFP}$ mice was severely, but not totally blocked at several stages of development in the BM. Thus, we performed further FACS analyses to assess whether reduced μHC expression also affected B-cell maturation or distribution of B-cell subsets in the spleen. B220 staining revealed a

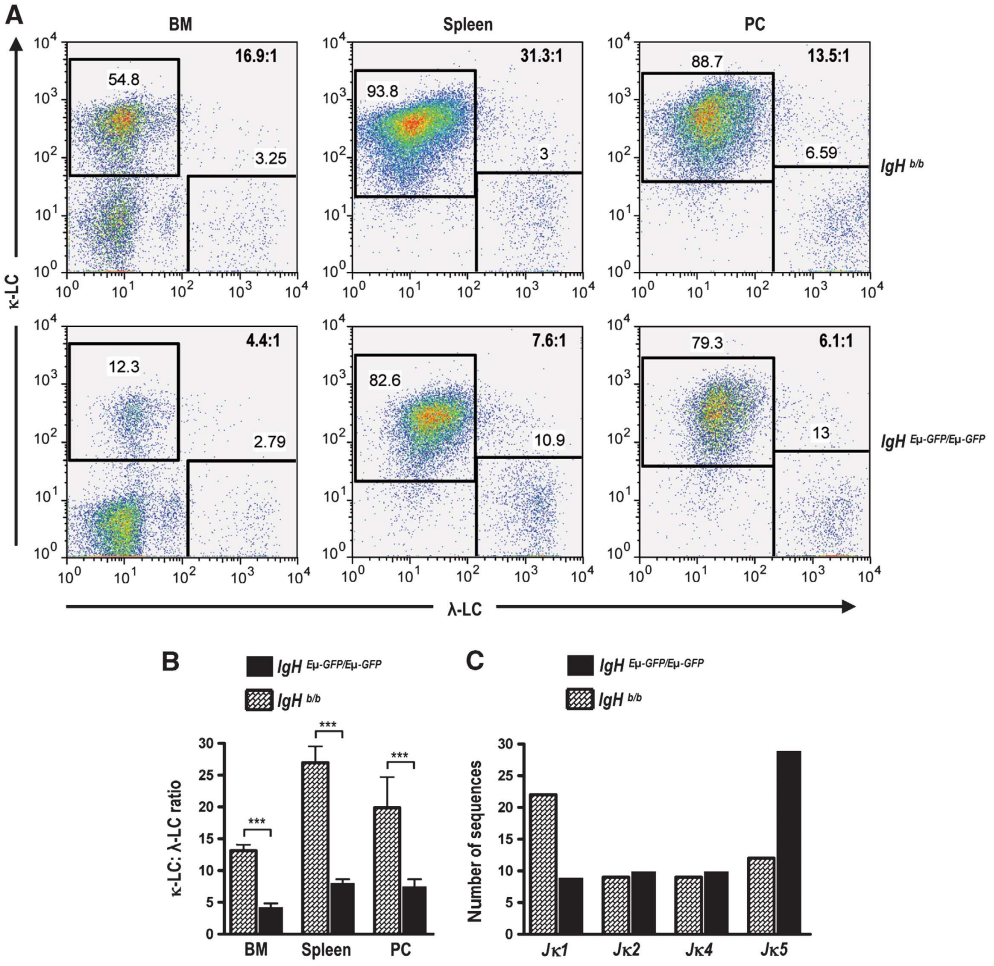

Figure 2 Enforced receptor editing in $IgH^{E\mu\text{-}GFP/E\mu\text{-}GFP}$ mice. (**A**) FACS analysis of κ-LC and λ-LC expression on $CD19^+$-gated lymphocytes from the BM, spleen and PC of WT and $IgH^{E\mu\text{-}GFP/E\mu\text{-}GFP}$ mice. Relative cell numbers are depicted within or above the gates and κ:λ-LC ratios are given on the upper right of each plot. (**B**) Ratios of κ-LC- to λ-LC-expressing B lymphocytes from WT and $IgH^{E\mu\text{-}GFP/E\mu\text{-}GFP}$ mice. Mean values and the s.e.m. of nine animals for each genotype are shown. $^{***}P<0.001$ (Mann-Whitney test). (**C**) Usage of different Jκ gene segments in purified $CD19^+$ splenic B cells from a WT and an $IgH^{E\mu\text{-}GFP/E\mu\text{-}GFP}$ mouse. In all, 52 (WT) and 58 ($IgH^{E\mu\text{-}GFP/E\mu\text{-}GFP}$) sequences bearing in-frame Vκ-Jκ rearrangements were considered.

highly significant 3- to 4-fold reduction in relative B-cell numbers of $IgH^{E\mu\text{-}GFP/E\mu\text{-}GFP}$ mice (Figure 3A and B, left panels). Moreover, most likely as a consequence of the developmental block in BM B-cell development, the fraction of CD93-expressing immature B lymphocytes in homozygous mutants was strongly diminished (Figure 3A and B). The pool of non-proliferating, immature B lymphocytes in the spleen can be further subdivided into three subsets by differential expression of CD23 and IgM (Allman *et al*, 2001). As indicated by the middle panels in Figure 3A and B, the distribution of transitional type 1 (T1), type 2 (T2) and type 3 (T3) B cells was barely altered in $IgH^{E\mu\text{-}GFP/E\mu\text{-}GFP}$ mice. Only the $CD23^+/IgM^{high}$ T2 transitional B-cell subset was slightly but significantly diminished in $IgH^{E\mu\text{-}GFP/E\mu\text{-}GFP}$ mice, suggesting that some T1 B cells in μHC-hypomorphic animals were not capable of developing into T2 B lymphocytes.

As determined by staining for CD21 and CD23, mutant mice exhibited a severe reduction of FO B cells both in relative as well as in absolute numbers (Figure 3A and B, right panels). Despite the relative increase of MZ B cells in $IgH^{E\mu\text{-}GFP/E\mu\text{-}GFP}$ mice, the absolute numbers of MZ B cells were not enlarged. We also measured the impact of reduced μHC mRNA synthesis on the resultant IgM protein expression in MZ B cells and FO B cells of $IgH^{E\mu\text{-}GFP/E\mu\text{-}GFP}$ mice. MZ B lymphocytes in mutant animals expressed clearly lower total μHC protein levels as compared with the WT controls whereas FO cells displayed only slightly reduced total μHC protein levels (Figure 3C). Similar results were obtained by staining for surface IgM. This rose the question to what extent both mature splenic B-cell subsets in $IgH^{E\mu\text{-}GFP/E\mu\text{-}GFP}$ mice were still capable of mediating adequate responses to BCR crosslinking. To test this, we measured the Ca^{2+} release of primary splenic B lymphocytes upon BCR stimulation with anti-IgM $F(ab')_2$ antibodies. As verified for nine mice of each genotype, the sustained but not the initial Ca^{2+} release in mutant MZ B lymphocytes was at all times lower than in corresponding WT cells being in line with the distinct reduction of both cytoplasmic and surface IgM levels observed for mutant MZ B cells. In contrast, calcium release in FO B cells was not altered significantly with the concentrations of anti-IgM $F(ab')_2$ antibodies used in the experiments (Figure 3D).

As $IgH^{E\mu\text{-}GFP/E\mu\text{-}GFP}$ mice displayed a clearly diminished ratio of FO to MZ B lymphocytes, we were interested in the splenic architecture of mutant animals. Both the quantity and

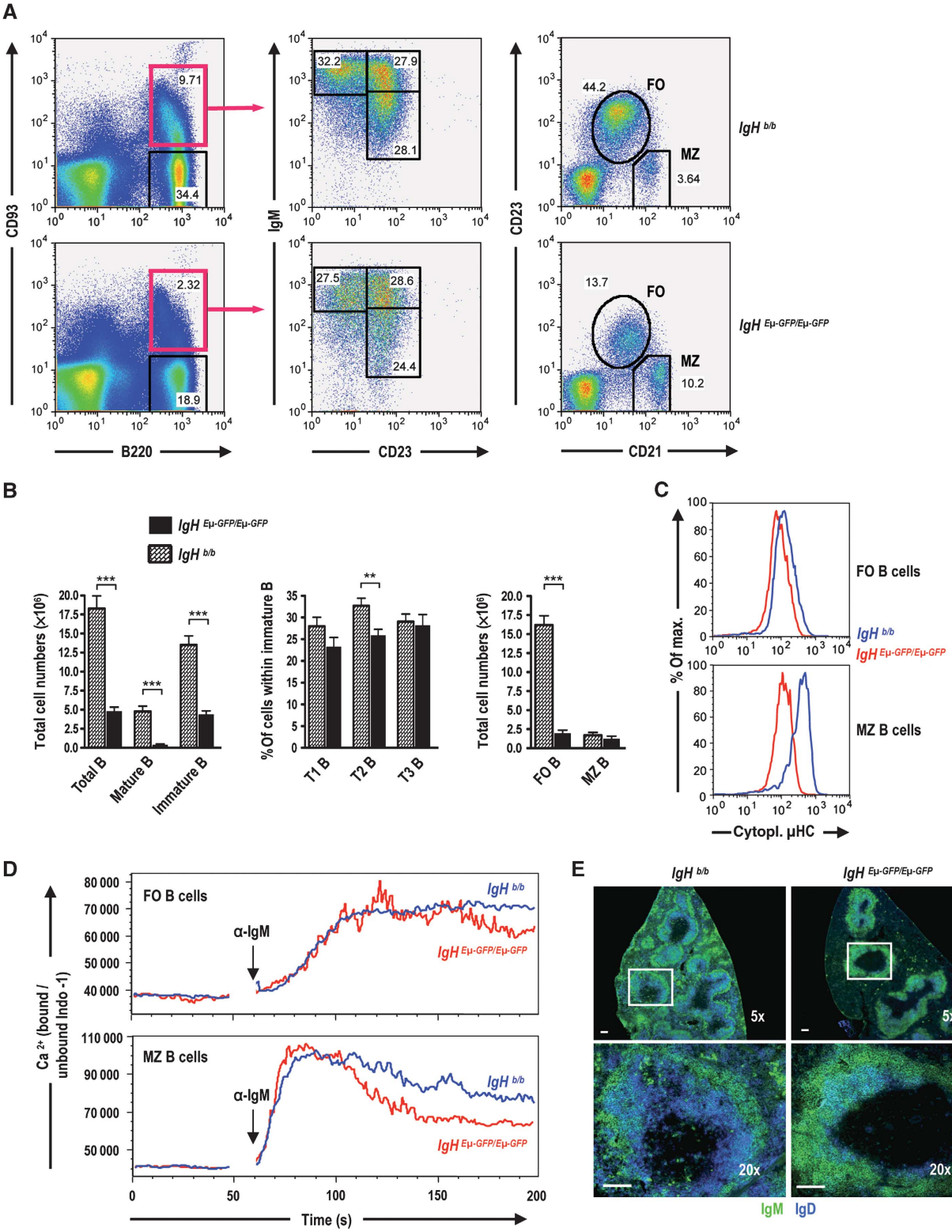

Figure 3 Effects of reduced μHC expression on splenic B cells. (**A**) Left: FACS analysis of B220 and CD93 surface expression on lymphocytes from WT and $IgH^{E\mu\text{-}GFP/E\mu\text{-}GFP}$ mice. Immature ($B220^+/CD93^+$) and mature ($B220^+/CD93^-$) B cells are depicted within the gates. Middle: Surface expression of CD23 and IgM on gated immature B cells. T1 ($CD23^-/IgM^{high}$), T2 ($CD23^+/IgM^{high}$) and T3 ($CD23^+/IgM^{int}$) B cells are differentiated. Right: Surface expression of CD21 and CD23 on $CD19^+$-gated B cells. FO ($CD21^{int}/CD23^{high}$) and MZ ($CD21^{high}/CD23^-$) B cells are shown. Relative cell numbers for indicated gates are given. (**B**) Statistics based on analyses from subfigure (**A**). Absolute numbers of total B, immature B and mature B cells, relative numbers of T1 B, T2 B and T3 B cells within the immature B-cell gate as well as total numbers of FO and MZ B cells are depicted. $^{**}P<0.01$; $^{***}P<0.001$ (Mann–Whitney test, $n>9$). (**C**) FACS of μHC expression in the cytoplasm of FO and MZ B cells from WT and $IgH^{E\mu\text{-}GFP/E\mu\text{-}GFP}$ mice ($n=3$). (**D**) Calcium responses of primary splenocytes stimulated with $F(ab')_2$ anti-IgM. Loading with Indo-1 was followed by staining for CD21 and CD23 to allow for gating for MZ and FO B cells. Representative data of nine experiments are shown. (**E**) Histology of spleens from naive WT and $IgH^{E\mu\text{-}GFP/E\mu\text{-}GFP}$ mice. Sections were stained with anti-IgM (green) and anti-IgD (blue). Original magnifications, $\times 5$ and $\times 20$. Scale bars, 100 μm. Data are representative of two mice for each genotype.

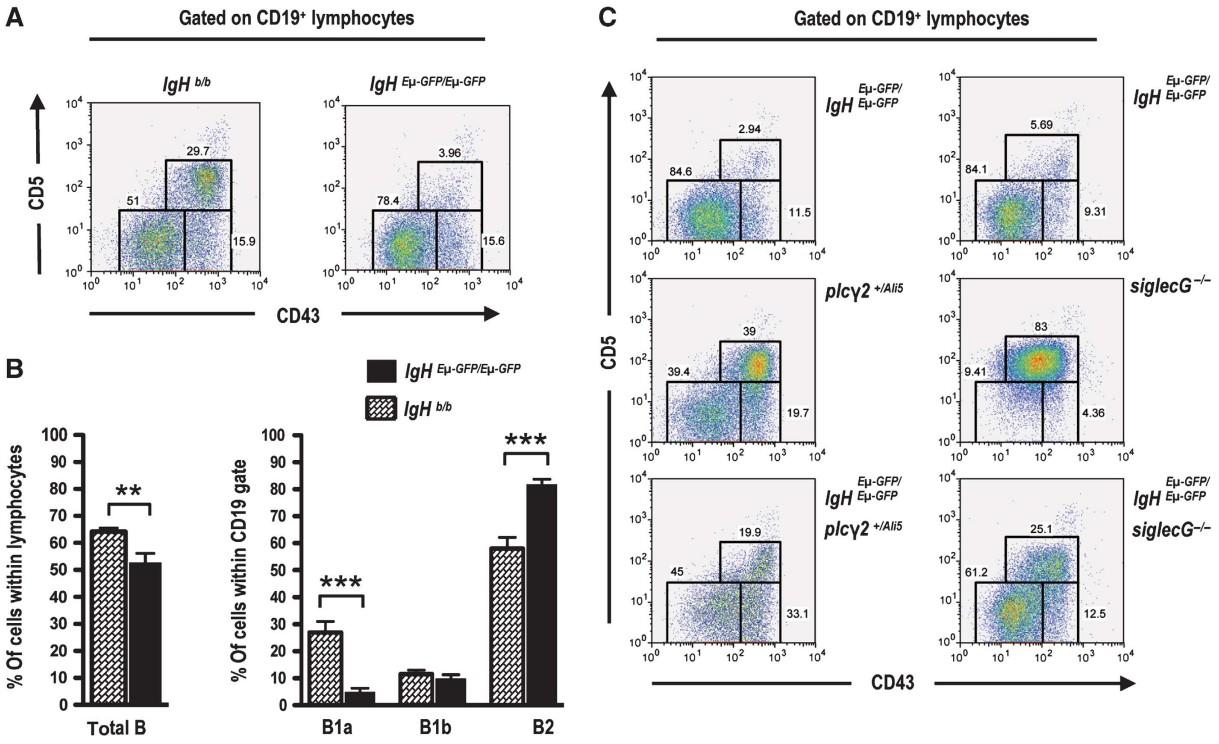

Figure 4 Impact of reduced μHC expression on B1-cell development in the PC. (**A**) FACS analysis of CD43 and CD5 surface expression on $CD19^+$-gated PC cells from WT and $IgH^{E\mu\text{-}GFP/E\mu\text{-}GFP}$ mice. B1a ($CD43^+/CD5^+$), B1b ($CD43^+/CD5^-$) and B2 ($CD43^-/CD5^-$) cells are depicted within gates. (**B**) Statistics based on analyses from subfigure (**A**). $CD19^+$ cells are designated total B cells. B1a, B1b and B2 cells are characterized as depicted in (**A**). Percentages of total B cells refer to the lymphocyte gate, percentages of B1a, B1b and B2 cells to the $CD19^+$-gate. Data are based on 11 mice of each genotype. $^{**}P<0.01$; $^{***}P<0.001$ (Mann–Whitney test). (**C**) Expression of CD43 and CD5 on $CD19^+$-gated cells from mice of the indicated genotypes. Severe reduction of B1a cells in $IgH^{E\mu\text{-}GFP/E\mu\text{-}GFP}$ mice is reversed by the $plc\gamma2^{+/Ali5}$ or the $siglecG^{-/-}$ mutation. Data are representative of three mice of each genotype.

size of white pulp areas were comparable in WT and mutant spleens. However, in line with the presented FACS data, considerably fewer FO B cells (IgM^{low}/IgD^{high}) were present in follicles of mutant mice (Figure 3E). MZs in mutant spleens had a normal size, supporting flow cytometric data, which revealed regular MZ B-cell (IgM^{high}/IgD^{low}) numbers in $IgH^{E\mu\text{-}GFP/E\mu\text{-}GFP}$ mice. Strikingly, extrafollicular IgM-secreting plasma cells (IgM^{high}) were almost completely absent in splenic sections from $IgH^{E\mu\text{-}GFP/E\mu\text{-}GFP}$ mice (Figure 3E).

Peritoneal B1a cells are severely reduced in $IgH^{E\mu\text{-}GFP/E\mu\text{-}GFP}$ mice

Studies with targeted mice either lacking negative or over-expressing positive regulators of BCR signalling suggest that the development of B1 cells appears to depend on strong BCR signals (Berland and Wortis, 2002). Our $IgH^{E\mu\text{-}GFP/E\mu\text{-}GFP}$ mice produce reduced μHC levels and therefore serve as an ideal model to study the impact of weak BCR signals on the emergence of B1 cells.

We performed FACS analyses to investigate whether overall B-cell numbers or the distribution of PC B-cell subsets were altered in $IgH^{E\mu\text{-}GFP/E\mu\text{-}GFP}$ mice. As determined by surface staining for CD19, relative numbers of B cells were slightly but significantly reduced in $IgH^{E\mu\text{-}GFP/E\mu\text{-}GFP}$ mice (Figure 4B). B1a-cell numbers were strongly reduced to about <20% in mutant mice coinciding with a relative expansion of B2 cells (Figure 4A and B). Interestingly, the size of the B1b ($CD43^+/CD5^-$)-cell subset was not significantly altered (Figure 4A and B).

PLCγ2 is a positive regulator of BCR signalling and targeted deletion of the corresponding gene was reported to result in decreased B1-cell numbers (Hashimoto *et al*, 2000; Wang *et al*, 2000). In $PLC\gamma2^{Ali5}$ mice (Yu *et al*, 2005), in which a point mutation results in prolonged membrane attachment of the mutant PLCγ2 protein and to stronger BCR-mediated Ca^{2+} signals, the B1-cell subset is increased. Thus, we mated $IgH^{E\mu\text{-}GFP/E\mu\text{-}GFP}$ mice with $PLC\gamma2^{Ali5}$ mice expecting that enforced BCR signals would result in a normalized distribution of B1a, B1b and B2 cells in the PC of double-mutant animals ($IgH^{E\mu\text{-}GFP/E\mu\text{-}GFP}/Plc\gamma2^{+/Ali5}$). In fact, $IgH^{E\mu\text{-}GFP/E\mu\text{-}GFP}$ mice with one mutated plcγ2 allele displayed higher numbers of B1a cells compared with $IgH^{E\mu\text{-}GFP/E\mu\text{-}GFP}$ mice carrying two WT alleles of plcγ2 (Figure 4C, left panel). Essentially, the distribution of B-cell subsets in the PC of double mutants resembled that found in WT mice (compare Figure 4A).

SiglecG-deficient mice exhibit a massive expansion of the B1a-cell population due to enforced Ca^{2+} signalling (Hoffmann *et al*, 2007). We mated $IgH^{E\mu\text{-}GFP/E\mu\text{-}GFP}$ with $SiglecG^{-/-}$ mice to assess whether reduced μHC expression would curtail the reported enlargement of the B1a subset. As illustrated in the right panel of Figure 4C, SiglecG-deficient $IgH^{E\mu\text{-}GFP/E\mu\text{-}GFP}$ mice actually displayed normalized levels of B1a, B1b and B2 cells, again resembling distributions found in WT mice. Interestingly, we did not observe an augmented appearance of B1a cells in spleens of SiglecG-deficient $IgH^{E\mu\text{-}GFP/E\mu\text{-}GFP}$ mice and splenic B-cell populations in $IgH^{E\mu\text{-}GFP/E\mu\text{-}GFP}$ mice were not affected by

SiglecG deficiency or one mutated plcγ2 allele (unpublished data).

Taken together, our findings show that altering the μHC levels and therefore constitutive BCR signalling strength directly impacts the development of the distinct peritoneal B-cell subsets. B1a cells are exclusively sensitive to reduced μHC levels and amplification of BCR signals is able to normalize B1a-cell numbers, suggesting a tight relationship between BCR signal strength and B1a-cell numbers.

Analysis of B-cell selection processes in competitive BM chimeras

To further analyse the developmental selection processes in μHC-hypomorphic B cells, we analysed the competence of BM cells from the homozygous mutants to reconstitute distinct B-cell subsets in competition with WT B cells in lethally irradiated Rag1$^{-/-}$ mice. Only 5% WT (IgH$^{b/b}$/Ly5.1^{+}) BM cells were mixed with 95% BM cells from IgH$^{Eμ\text{-}GFP/Eμ\text{-}GFP}$ mice to give mutant precursors a competitive advantage (Figure 5). To test for the adequacy of haematopoietic reconstitution, we initially checked the expression of Ly5 allotypes on T cells in spleen and PC of mixed chimeras. Only 2.3 ± 0.4 and 2.6 ± 0.4% of T lymphocytes (spleen and PC, respectively; mean ± s.e.) expressed the Ly5.1 marker reflecting the relative contribution of WT cells to the compartments not affected by the targeted mutation of the μHC locus. Pro-B cells of WT origin were slightly less contributing to the pro-B-cell compartment as compared with the T-cell contribution (1.9 ± 0.8%), supporting the view that differentiation into the B-cell lineage is not altered in IgH$^{Eμ\text{-}GFP/Eμ\text{-}GFP}$ progenitors. In the large pre-B-cell compartment, however, the contribution of WT cells is already ~5- to 6-fold higher (10.6 ± 3.8%), further substantiating the strong impact of hypomorphic μHC expression on the pre-B-cell checkpoint in the BM. Among small pre-B cells, a similar percentage of WT cells was found (9.1 ± 3.9%), suggesting no influence of hypomorphic μHC expression on this differentiation step of BM B lymphopoiesis. The developmental block at the pre-B to immature B-cell stage in IgH$^{Eμ\text{-}GFP/Eμ\text{-}GFP}$ mice is further corroborated by the higher contribution of WT immature B cells in the BM (16.8 ± 5.5%) as compared with small pre-B cells. Among the recirculating mature B cells in the BM, cells from WT origin are strongly enriched (42.0 ± 6.2%).

In the spleen, the percentage of immature B cells of WT origin was comparable to the percentage of immature B cells of WT origin in the BM (15.6 ± 3.6 versus 16.8 ± 5.5%, respectively; Figure 5, middle panel), indicating no influence of hypomorphic μHC expression on selection events at the egress from the marrow to distant spleen sites. Despite reconstituting only 15% of the immature B-cell compartment in the spleen, WT cells constituted about 50% of the mature splenic B-cell compartment in the mixed BM chimeras, suggesting a strong influence of hypomorphic μHC expression on positive selection into the mature B-cell pool.

As it has been proposed that BCR signalling strength is involved in lineage commitment of splenic B cells (Pillai *et al*, 2004), we were interested in the question, whether differences in tonic BCR signal strength are also involved in FO versus MZ B-cell development. As displayed in Figure 5 (middle panel), the BM chimeras provide clear evidence that μHC-hypomorphic cells contributed less to the MZ B-cell subset as compared with FO B cells (38.4 versus 57.4%, $P<0.001$). This result suggests that selection processes for MZ B cells are more sensitive to reduced μHC expression as compared with FO B cells.

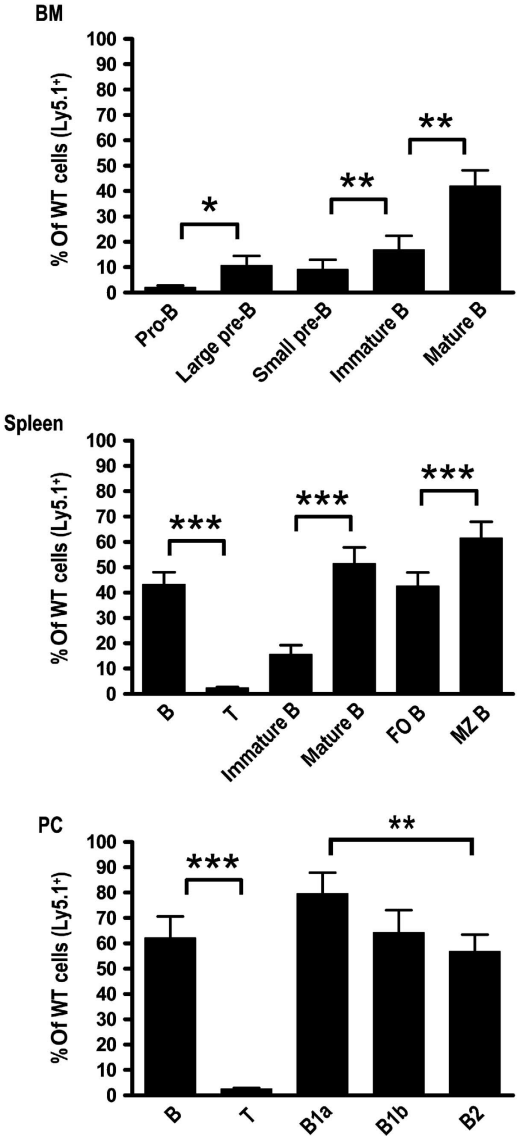

Figure 5 Analysis of IgH$^{Eμ\text{-}GFP/Eμ\text{-}GFP}$ B-cell development in competitive BM chimeras. Contribution of WT (Ly5.1^{+}) cells to the given cell populations in BM (top), spleen (middle) and PC (bottom) of mixed BM chimeras. Mixtures of 5% WT BM (Ly5.1^{+}) and 95% BM (Ly5.2^{+}) from IgH$^{Eμ\text{-}GFP/Eμ\text{-}GFP}$ mice were injected into lethally irradiated Rag-1$^{-/-}$ mice. Depicted are the mean percentages + s.e.m. ($n=7$–9) of Ly5.1^{+} cells in the different populations. Analysed cell subsets within the lymphocyte gate were defined by the following combinations of cell surface markers. BM: pro-B, B220^{+}/ckit^{+}; pre-B, B220^{+}/CD25^{+} (large, FSC^{high}; small, FSC^{low}); immature B, B220^{low}/IgM^{int}; mature B, B220^{high}/IgM^{int}. Spleen: total B, B220^{+}/CD3^{-}; total T, B220^{-}/CD3^{+}; immature B, B220^{+}/CD93^{+}; mature B, B220^{+}/CD93^{-}; FO B, CD21^{int}/CD23^{+}; MZ B, CD21^{high}/CD23$^{low/-}$. PC: total B, B220^{+}/CD3^{-}; total T, B220^{-}/CD3^{+}; B1a, B220^{+}/CD43^{+}/CD5^{+}; B1b, B220^{+}/CD43^{+}/CD5^{-}; B2, B220^{+}/CD43^{-}/CD5^{-}. *$P<0.05$; **$P<0.01$; ***$P<0.001$ (Wilcoxon matched pairs test).

When we analysed the distinct B-cell subsets in the PC of mixed BM chimeric mice, we found that IgH$^{Eμ\text{-}GFP/Eμ\text{-}GFP}$ cells reconstituted B2, B1b and B1a cells with decreasing frequencies, respectively. The contribution of WT cells to the B1a

compartment was significantly higher than to the B1b compartment (79.6 ± 8.3 versus 64.2 ± 8.9%, $P<0.001$), whereas the WT contribution of B2 cells in the PC was in the range of mature splenic B cells (56.7 ± 6.7%; Figure 5, bottom panel).

Taken together, the analyses on mixed BM chimeras further supported our findings from homozygous $IgH^{E\mu\text{-}GFP/E\mu\text{-}GFP}$ mice. At several stages of development, mutant B cells with hypomorphic μHC expression failed to effectively compete with WT B cells. Given an effective percentage of only ~2.5% of BM stem cells in the chimeras, WT B lymphopoiesis resulted in ~20-fold better reconstitution of the mature splenic B-cell pool and ~30-fold better reconstitution of the B1a-cell pool.

Reduced levels of BAFF receptor on splenic B cells in IgH$^{E\mu\text{-}GFP/E\mu\text{-}GFP}$ mice

Continuous signals from both the BCR as well as the receptor for B-cell activating factor (BAFF) (BAFF-R) are necessary for survival of peripheral B-cell subsets (Cancro, 2009). As we noted a strong influence of hypomorphic μHC expression on positive selection into the mature B-cell pool we measured the expression levels of BAFF-R on splenic B-cell subpopulations. As depicted in Figure 6A, BAFF-R expression was consistently found to be lower on immature as well as FO and MZ cells in the spleen of $IgH^{E\mu\text{-}GFP/E\mu\text{-}GFP}$ mice. In addition, both FO as well as MZ cells from $IgH^{E\mu\text{-}GFP/E\mu\text{-}GFP}$ mice responded to BAFF with significantly lower survival *in vitro* (Figure 6B). Interestingly, survival curves in culture medium without BAFF were indistinguishable between WT and $IgH^{E\mu\text{-}GFP/E\mu\text{-}GFP}$ FO and MZ cells. It has been described that treatment with BAFF increases B-cell size (Patke *et al*, 2006). We therefore compared the increase of B-cell size by BAFF treatment *in vitro*. As shown in Supplementary Figure S5, B cells from $IgH^{E\mu\text{-}GFP/E\mu\text{-}GFP}$ mice responded to BAFF treatment with a reduced increase in cell size as measured by forward scatter characteristics. Taken together, our data suggest that hypomorphic BCR expression results in lower expression of BAFF-R in peripheral B-cell subpopulations and a concomitant lower survival rates in response to BAFF.

Reduced immunoglobulin levels and impaired antibody responses in IgH$^{E\mu\text{-}GFP/E\mu\text{-}GFP}$ mice

B1 cells continuously secret immunoglobulins without being exposed to specific antigen and are therefore the main source of 'natural IgM' in sera of naive mice (Martin and Kearney, 2001; Berland and Wortis, 2002). Thus, we asked if levels of

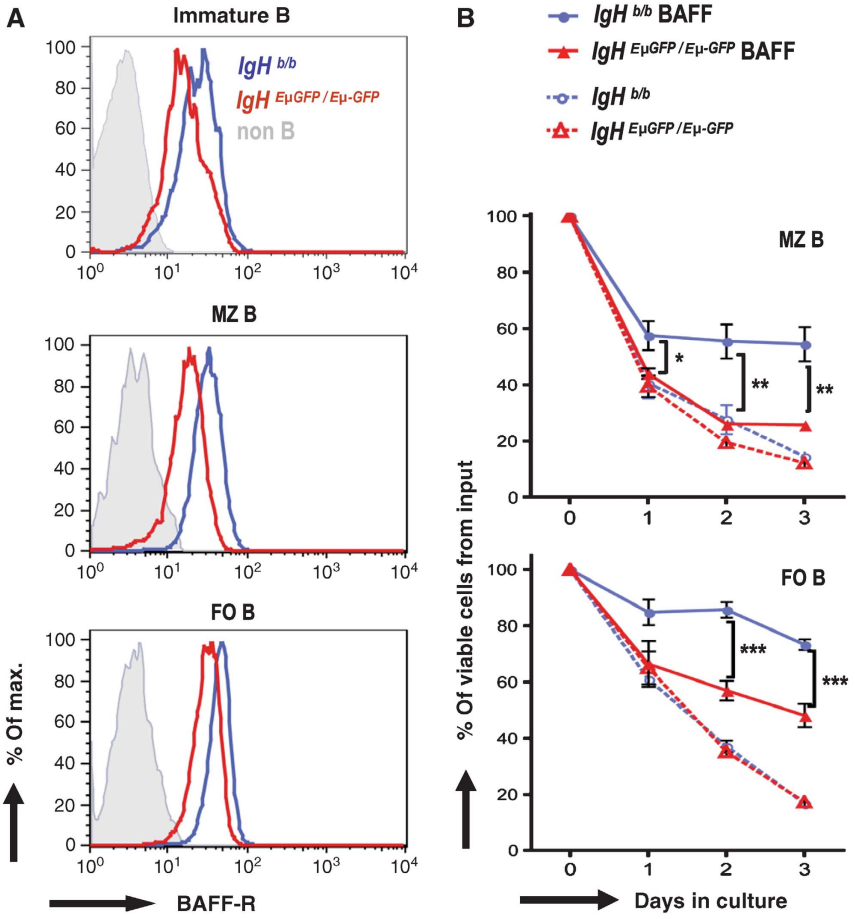

Figure 6 BAFF-R levels and BAFF responsiveness of $IgH^{E\mu\text{-}GFP/E\mu\text{-}GFP}$ B cells in the spleen. (**A**) BAFF-R expression is shown for immature ($CD93^+$, $B220^+$), FO ($B220^+$, $CD21^{int}$, $CD23^+$) and MZ ($B220^+$, $CD21^{high}$, $CD23^-$) B cells. Shaded histograms show staining levels on non-B cells. The data are representative of four independent experiments. (**B**) Sorted FO and MZ B cells from spleen were cultured in the absence and presence of 200 ng/ml BAFF. Viable cells were counted every day for 3 days. Blue circles denote WT cells, red triangles mutant cells; open symbols denote cultures without BAFF, filled symbols cultures with BAFF (200 ng/ml). Mean values ± s.e.m. are shown from four (FO) and two (MZ) independent experiments with duplicate cultures. $^*P<0.05$; $^{**}P<0.01$; $^{***}P<0.001$ (Mann–Whitney test).

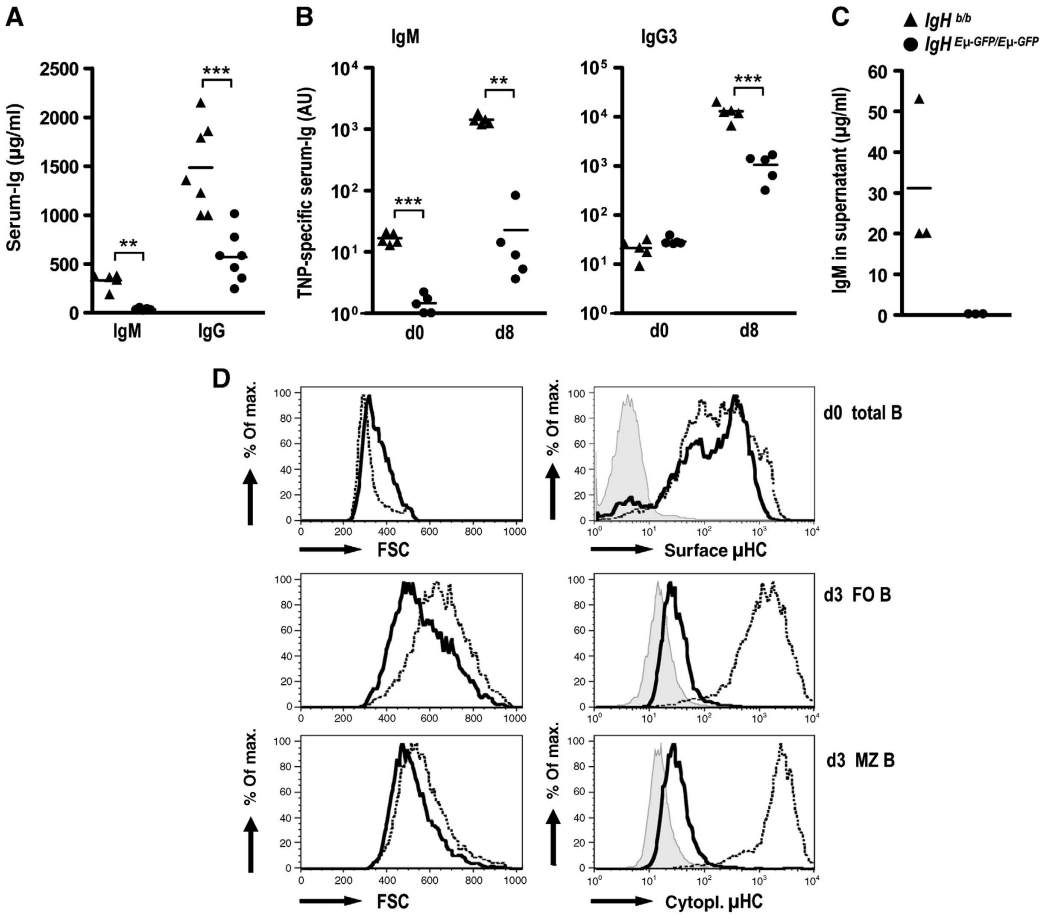

Figure 7 Reduced serum immunoglobulin levels and constricted immune responses in $IgH^{E\mu\text{-}GFP/E\mu\text{-}GFP}$ mice. (**A**) ELISA of immunoglobulin serum titres in naive WT and $IgH^{E\mu\text{-}GFP/E\mu\text{-}GFP}$ mice. (**B**) ELISA of specific antibody responses in WT and $IgH^{E\mu\text{-}GFP/E\mu\text{-}GFP}$ mice upon immunization with the TI-2 antigen TNP-Ficoll. AU, arbitrary units. (**C**) IgM levels in the supernatant (200 µl medium) of 5×10^4 B cells 4 days after stimulation with 10 µg/ml LPS were measured by ELISA. Each symbol in (**A**–**C**) represents one mouse. (**D**) FACS analysis of FSC characteristics (left panels) of unstimulated (d0; upper panels) and LPS stimulated (d3; middle and lower panels) sorted FO and MZ cells and of surface (upper panel) and cytoplasmic (middle and lower panels) IgM expression (right panels). WT mice: dotted lines; $IgH^{E\mu\text{-}GFP/E\mu\text{-}GFP}$ mice: thick lines; grey shaded histograms: isotype control staining. Data are representative of three mice of each genotype.

serum IgM were altered in $IgH^{E\mu\text{-}GFP/E\mu\text{-}GFP}$ mice as a consequence of the severely decreased B1a-cell numbers. In fact, we observed an ~10-fold reduction of natural IgM as determined by ELISA (Figure 7A). The strongly diminished numbers of extrafollicular IgM-secreting plasmablasts and plasma cells in the spleen might additionally account to this phenotype (Figure 3E). Levels of natural IgG were less affected, being reduced about three-fold in mutant mice (Figure 7A).

To characterize immune responses, we first injected WT and $IgH^{E\mu\text{-}GFP/E\mu\text{-}GFP}$ mice with the thymus-independent type 2 (TI-2) antigen trinitrophenol (TNP)-ficoll. Natural TNP-specific IgM was undetectable in sera of naive $IgH^{E\mu\text{-}GFP/E\mu\text{-}GFP}$ mice and specific IgM responses resulted in ~100-fold lower titres at day 8 after immunization when compared with WT controls (Figure 7B, left panel). TNP-specific IgG3 antibodies were reduced ~10-fold after immunization (Figure 7B, right panel). These results were unexpected, as MZ B cells have been shown to be the major responding B-cell subpopulation to TI-2 antigens (Martin *et al*, 2001) and absolute MZ B lymphocyte numbers were normal in the mutant mice (Figure 4B).

Therefore, we analysed antibody secretion of mutant B cells *in vitro* upon stimulation with LPS. Remarkably, IgM production by $IgH^{E\mu\text{-}GFP/E\mu\text{-}GFP}$ B cells was undetectable (Figure 7C) despite apparently normal activation and proliferation of µHC-hypomorphic cells (Figure 7D). B cells from $IgH^{E\mu\text{-}GFP/E\mu\text{-}GFP}$ mice showed increased cell size 3 days after activation with LPS, indicating regular activation (Figure 7D). Staining for cytoplasmic µHC, however, revealed almost absent cytoplasmic µHC protein in LPS blasts from $IgH^{E\mu\text{-}GFP/E\mu\text{-}GFP}$ mice (Figure 7D), which was also confirmed by western blot analysis (Supplementary Figure S6).

These findings led us to hypothesize that during plasma cell differentiation of mutant B cells the pA machinery is preferentially directed to the strong SV40 pA sites downstream of the gfp-cassette, which have been introduced by gene targeting and thereby creating truncated µHCs. It has recently been shown that enhanced loading of the transcription elongation factor ELL2 and the polyadenylation factor CstF-64 on RNA polymerase II upon plasma cell differentiation causes enhanced use of the proximal pA site of the secretory form of IgH (Martincic *et al*, 2009). In case of the $IgH^{E\mu\text{-}GFP}$ allele, the SV40 pA site of the gfp-cassette is the most proximal pA site, providing a possible explanation for severely reduced cytoplasmic µHC levels during plasma cell differentiation. Indeed, QPCR analysis revealed an ~12-fold

reduction of J_H2-Cμ1 mRNA levels in LPS blasts from $IgH^{Eμ\text{-}GFP/Eμ\text{-}GFP}$ mice as compared with WT mice (Supplementary Figure S7), whereas J_H2-Cμ1 mRNA levels were only modestly reduced in unstimulated splenic B cells (Table I). The mRNA levels of κ-LCs were even enhanced in mutant LPS blasts (Supplementary Figure S7). We, therefore, propose that the preferential usage of the introduced pA site is mainly responsible for strongly impaired antibody secretion in $IgH^{Eμ\text{-}GFP/Eμ\text{-}GFP}$ mice.

Discussion

It is widely accepted that development and positive selection of B lymphocytes depends on the quality and quantity of signals generated by their pre-BCRs and BCRs and that signalling strength is also involved in B-lymphocyte lineage decisions (Niiro and Clark, 2002; Casola *et al*, 2004). These notions evolved from plenty of studies dealing with gene-targeted mice, which lack positive or negative regulators of BCR signalling or alternatively overexpress particular signalling components. As most signalling components of the BCR have diverse functions and are involved in other signalling pathways, as exemplified for the syk tyrosine kinase (Kulathu *et al*, 2009) the reported phenotypes can rarely be attributed to altered signalling strength of the BCR alone. This is even more complicated in downstream components of the signalling machinery, for example, for the NF-κB signalling pathway (Derudder *et al*, 2009). Here, we describe a unique and novel mouse mutant in which attenuated receptor signals in both developing and mature B-cell subsets resulted only from the global reduction of μHC mRNA and hence μHC protein levels. Any receptors and regulators involved in pre-BCR and BCR signalling pathways remained intact.

The first checkpoint in B-cell development in which signals downstream of the μHC are involved in positive selection occurs when pre-BCR signalling induces a burst of proliferation, which increases the number of cells that have successfully recombined their IgH genes (reviewed in Herzog *et al* (2009)). The 5- to 6-fold reduction of mutant large pre-B cells in competitive BM chimeras supports the notion that the strength of pre-BCR signalling quantitatively affects the proliferation of pre-B cells. This is in accordance with the suggested repertoire selection model (Melchers, 2005; Vettermann *et al*, 2006), in which the pairing capacity of μHCs with the SLC controls the density of surface pre-BCR levels and therefore the magnitude of signals for proliferation and clonal expansion.

B-cell development in the BM of $IgH^{Eμ\text{-}GFP/Eμ\text{-}GFP}$ mice was partially blocked at the transition from pre-B to immature B cells accompanied by enforced secondary LC rearrangements. According to a hypothetical receptor editing model (Nemazee and Hogquist, 2003), signalling through newly formed BCRs below a certain threshold would be insufficient to downregulate Rag genes leading to maturation arrest and ongoing LC recombination. The results from $IgH^{Eμ\text{-}GFP/Eμ\text{-}GFP}$ mice described here directly support this model. Appropriate basal or 'tonic' signals have to be provided from BCRs in immature B cells to downregulate Rag gene expression and to suppress further LC rearrangement as shown here for the first time in mice carrying a diverse B-cell repertoire and normal levels of all B-cell signalling components. Our findings that immature B cells from mutant and WT mice show similar Rag-2 expression can be interpreted as a result of undetectable surface expression of IgM in 'pre-B-like' cells that undergo LC editing. Cells that express a detectable BCR apparently have downregulated Rag expression to a similar extend in WT and mutant mice.

The signalling strength of the BCR at the immature B-cell stage is critical for development of the three functionally distinct mature B-cell populations (Hardy *et al*, 2007). There has been an ongoing debate concerning origin and developmental progression of both populations. Recently, a specific B1-cell progenitor was identified, which primarily appeared in fetal tissue but still could be detected in adult BM (Montecino-Rodriguez *et al*, 2006) providing strong evidence for the so-called 'lineage-model' of B1- and B2-cell emergence (reviewed in Dorshkind and Montecino-Rodriguez (2007)). Nevertheless, genetic alterations leading to increased BCR signalling strength generally favour B1-cell development (reviewed in Berland and Wortis (2002)) and in BCR-transgenic mice increasing BCR surface density also results in elevated B1-cell levels (Lam and Rajewsky, 1999; Watanabe *et al*, 1999). Moreover, targeted mice carrying the Epstein-Barr virus protein LMP2A as BCR surrogate almost exclusively developed B1-like cells, when LMP2A was under transcriptional control of a strong promoter. In case of weak LMP2A expression, B1-like cells were completely absent (Casola *et al*, 2004). Thus, the B1 versus B2 cell fate decision seems to depend on BCR signalling strength regardless of the receptor specificity. Since our μHC-hypomorphic mice exhibit severely reduced levels of B1 cells, they are further evidence for the 'selection-theory', whereupon B1-cell development requires a certain threshold of BCR signalling at the $sIgM^+$ stage (Lam and Rajewsky, 1999; Berland and Wortis, 2002). In line with the latter model, elevated Ca^{2+} signals in $IgH^{Eμ\text{-}GFP/Eμ\text{-}GFP}$ mice achieved by deletion of SiglecG or by a gain of function mutation in PLCγ2 notably reversed the strong reduction of B1a cells in these animals to approximately WT levels. Taken together, there is now sufficient evidence for both the 'lineage-model' and the 'selection-theory'. Thus, we would favour a combined model, according to which B1 cells develop from a distinct progenitor but still need strong signals for further developmental progression and maturation (Montecino-Rodriguez *et al*, 2006). Additionally, high surface densities of IgM and CD19 observed for WT B1 cells would perfectly match this model with both molecules accounting for strong BCR-mediated signals.

Interestingly, numbers of B1b cells are almost unaffected by lower BCR levels in our μHC-hypomorphic mice, further supporting the notion that the two B1 sister populations have distinct functions. B1b cells are considered to be induced after antigenic exposure and are essential for protective antibodies against certain pathogens such as *Streptococcus pneumoniae* and *Borrelia hermsii* (Alugupalli *et al*, 2004; Haas *et al*, 2005).

Tonic signalling by the BCR is required for the survival of peripheral immature as well as MZ and FO B cells (Kraus *et al*, 2004). In addition, however, signals from the BAFF-R are equally important for positive selection and survival of mature B-cell populations as substantiated by higher B-cell numbers in BAFF-transgenic animals and substantially lower B-cell numbers in BAFF-deficient mice (Mackay and Schneider, 2009). Our data presented here suggest that lower BCR levels which presumably result in lower tonic BCR signalling affect BAFF-R expression levels in immature

as well as mature splenic B lymphocytes. It has been described that the BAFF-R is upregulated in late transitional and mature B cells after BCR crosslinking (Smith and Cancro, 2003). Our findings here significantly extend these findings to constitutive BCR signals without BCR crosslinking and provide further evidence for extensive cross-modulation of BCR- and BAFF-signalling pathways (Cancro, 2009). As lower levels of BAFF-R translated in less survival signals after BAFF treatment in hypomorphic IgM B cells *in vitro*, it can be expected that lower BAFF-R levels are also responsible for the lower competitiveness of B cells from the mutant mice in direct competition with WT B cells *in vivo*.

It was postulated that BCR signalling strength also impacts the MZ versus FO B-cell decision in a way that MZ B cells would develop from precursors with poor BCR signals, whereas differentiation into the FO B lineage would be due to 'intermediate' signals (reviewed in Pillai *et al* (2005)). At first glance, elevated MZ B-cell percentages in the spleen of $IgH^{E\mu\text{-}GFP/E\mu\text{-}GFP}$ mice would be in accordance with this model. However, absolute MZ B-cell numbers were found to be normal. The same phenomenon was described for many transgenic and knockout mice with lymphocytopaenia, as exemplified in $\lambda5^{-/-}$ mice (Harfst *et al*, 2005). The observation that the MZ B-cell pool in the spleen is kept at normal levels when the influx from the BM was experimentally stopped (Hao and Rajewsky, 2001), suggested self-renewal of MZ B cells. We propose that in situations with restricted generation of B cells, like in the $IgH^{E\mu\text{-}GFP/E\mu\text{-}GFP}$ mice presented here, a normal MZ B-cell compartment is established over time and remains constant once the compartment is filled. The analysis of competitive BM chimeras clearly showed that among the mature splenic B-cell subpopulations the MZ B-cell pool is affected even stronger by the hypomorphic IgH mutation than the FO B-cell pool.

The analysis of *in vitro* and *in vivo* antibody secretion in $IgH^{E\mu\text{-}GFP/E\mu\text{-}GFP}$ mice revealed a severe impairment, particularly for IgM antibodies. We suggest that this phenomenon is primarily explained by the preferential usage of the first available pA site by the travelling RNA polymerase II intensely loaded with ELL2 and CstF-64 in plasma cells. Due to intense loading of the elongation complex with CstF-64, Ig mRNA is preferentially cut at the first available pA site (Martincic *et al*, 2009). At a WT IgH locus, the secretory-specific immunoglobulin pA site is the most promoter-proximal pA site. In contrast, at the targeted $IgH^{E\mu\text{-}GFP}$ locus the pA site in the intron between VDJ and the Cμ1 exon is the most proximal site. The preferential usage of this signal likely leads to transcripts lacking all Cμ or Cγ segments and neither membrane-bound nor secreted Ig would be expressed in plasma cells of $IgH^{E\mu\text{-}GFP/E\mu\text{-}GFP}$ mice. Thus, our mouse model offers the opportunity to study plasma cell differentiation in the absence of the upregulation and accumulation of μHC in the endoplasmic reticulum, which is believed to be responsible for the induction of the unfolded protein response in activated B cells (Iwakoshi *et al*, 2003).

Materials and methods

Generation of the targeting construct and of $IgH^{E\mu\text{-}GFP/E\mu\text{-}GFP}$ mice

Details of the generation of the targeting construct and of the mutant mice are provided in the Supplementary data.

Mice

All mice were bred and maintained under specific pathogen-free (SPF) conditions in the mouse facility of the University of Erlangen. Mice in each experiment were age matched and mostly littermates. All animal experiments were carried out according to valid project licenses, which were approved by the local Veterinary Authorities.

Analysis of μHC mRNA levels

Pre-B, MZ B and FO B cells were sorted with a MoFlo cell sorter (Cytomation) and analysed for purity using a FACSCalibur (BD). mRNA from purified cells was isolated using the RNeasy-Kit (Qiagen) and reverse transcribed to cDNA with SuperScript II Reverse Transcriptase (Invitrogen). Quantitative RT–PCR (QPCR) was performed with Absolute QPCR SYBR Green Fluorescein Mix (ABgene) in an iCycler iQ (Bio-Rad). An initial 1:5 dilution of cDNAs in H_2O and further six 1:2 dilutions thereof were applied. Reactions with each dilution were run in duplicates and mean C_T values were calculated thereof. Relative cDNA levels were normalized to the housekeeping gene β-actin. The following primers were used for QPCR:

5′-ACCACTCTCACAGTCTCCTCAGA-3′ (J_H2.0_forw),
5′-GCTATGGACTACTGGGGTCAAG-3′ (J_H4.1_forw),
5′-CAAGGAACCTCAGTCACCGTCT-3′ (J_H4.2_forw),
5′-CAGTGTTGGGAAGGTTCTGATAC-3′ (C_μ1_rev),
5′-AATCCTGTGGCATCCATGAAAC-3′ (β-actin_forw) and
5′-CGCAGCTCAGTAACAGTCCG-3′ (β-actin_rev).

Flow cytometry

Single-cell suspensions of BM, spleen and from PC lavages were prepared. In all, 1×10^6 cells were incubated for 30 min at 4°C with the indicated reagents in PBS supplemented with 2% FCS, 0.05% azide and 2 mM EDTA (EDTA was not supplemented when incubating with α-CD93) at saturating conditions. Intracellular staining was done with a Fix&Perm kit (ADG) according to the manufacturers instructions subsequent to surface staining. Flow cytometry data were collected with a FACSCalibur (Becton Dickinson) and analysed with FlowJo software. Following antibodies and secondary reagents were used in this study: α-B220-FITC or -PerCP, α-IgM-bio, α-IgM^a-FITC, α-CD23-PE or -bio, α-IgκLC-PE, α-$\lambda_1/_2$LC-FITC and α-CD45.1-FITC were all purchased from BD. α-B220-APC, α-CD19-AF647, α-IgD-bio, α-CD23-FITC, α-CD25-PE, α-ckit-PE, α-CD93-bio, α-CD21/CD35-FITC, α-CD43-FITC, α-CD5-PE, α-CD3-bio, α-BAFF-R-FITC, α-CD45.1-Cy5 and α-CD45.2-APC were purchased from eBioscience. Anti-IgM (μHC-spec.)-FITC or -Cy5, Streptavidin-PE or -Cy5 were purchased from Jackson.

Calcium measurements in primary mouse cells

A total of 3×10^6 splenocytes were incubated with 1 μg/ml of Indo-1 (Invitrogen) and 0.15 μg/ml of pluronic F-127 (Invitrogen) in IMDM supplemented with 5% FCS at 30°C for 25 min. An equal volume of IMDM supplemented with 10% FCS was then added followed by a 10-min incubation step at 37°C. Subsequent extracellular staining was accomplished with α-CD21/CD35-FITC and α-CD23-PE. After two washing steps in Ringer solution, cells were stimulated with 12.5 μg/ml of $F(ab')_2$ anti-IgM (Jackson) in Ringer solution. Calcium flux was measured with the LSRII (Becton Dickinson). Equal loading of the samples with Indo-1 was controlled by treating cells with 100 nM ionomycin (Sigma). Raw data files were transferred to FlowJo software and are presented as median in comparative overlays.

Analysis of Jκ usage

Splenocytes were magnetically sorted with α-CD19 microbeads (Miltenyi) and purity of B cells was checked by staining with APC-labelled α-B220. mRNA isolation and reverse transcription was carried out as described above. Degenerate Vκ-framework-3 (5′-AGCTTCAGTGGCAGTGGRTCWGGRAC-3′) and Cκ (5′-CTTCCAC TTGACATTGATGTC-3′) primers were used for PCR amplification. Resulting VκJκCκ fragments were cloned into the Strataclone PCR cloning vector (Agilent) and single colonies were sequenced using the T7 primer (5′-CCTATAGTGAGTCGTATTAC-3′) to determine the Jκ in each. Sequence analysis was carried out with the Ig Blast program.

Mixed and WT BM chimeras

$Rag1^{-/-}$ mice were used as recipients and therefore lethally irradiated with 9 Gy. Within 24 h donor BM cells were isolated

from Ly5.2$^+$ IgH$^{E\mu\text{-}GFP/E\mu\text{-}GFP}$ mice and from Ly5.1$^+$ WT mice. After lysis of erythrocytes donor BM cells were treated with an α-CD4/α-CD8 hybridoma supernatant and incubated for 10 min at 37°C. Lyophilized LOW-TOX M rabbit complement (Cedarlane, Canada) was added to kill T cells. Thereafter, cells were incubated at 37°C for another 45 min. Remaining splenocytes were purified by Ficoll gradient. Rag1$^{-/-}$ mice either received a mixture of 95% Ly5.2$^+$ IgH$^{E\mu\text{-}GFP/E\mu\text{-}GFP}$ cells and 5% Ly5.1$^+$ WT cells or alternatively 100% Ly5.1$^+$ WT cells with the latter mice serving as controls. A total of 5×10^6 cells per mouse were injected intravenously. Mice were sacrificed no earlier than 8 weeks after transplantation and cells from BM, spleen and PC were analysed by flow cytometry. Origin and composition of lymphocytes were determined by means of α-CD45.1 and α-CD45.2 alloantigenic markers.

Cell culture

Recombinant mouse BAFF was purchased from Alexis Biochemicals. FACS-sorted B cells were cultured at 1×10^5–1×10^6 cells/ml in RPMI supplemented with 10% FCS, 50 μM β-mercaptoethanol, 2 mM glutamine, 100 U/ml penicillin and 100 mg/ml streptomycin in the presence or absence of 200 ng/ml BAFF. Cell viability was assessed following staining with propidium iodine by flow cytometry. Live cell numbers were quantified using TruCount reference microbeads (Becton Dickinson) and cell size was measured by forward light scatter.

Immunization and ELISA

Age-matched mice were immunized intravenously once on day 0 with a total of 15 μg TNP-Ficoll per mouse. Sera were taken at indicated time points. ELISA studies with sera from naive and immunized mice were carried out using techniques as described (Hoffmann *et al*, 2007).

Histology

Cryosections were prepared, stained and analysed exactly as described earlier (Hebeis *et al*, 2004).

Statistical analysis

Statistical significance was calculated with the Mann–Whitney test or the Wilcoxon matched pairs test when paired data sets were analysed using Prism (Graphpad Software Inc., La Jolla, CA, USA).

Supplementary data

Supplementary data are available at *The EMBO Journal* Online (http://www.embojournal.org).

Acknowledgements

We would like to thank Veronika Lodermeyer for help in performing Jκ-usage experiments; Andrea Schneider and Markus Mroz for expert technical assistance; Uwe Appelt for cell sorting and Jasmin Horlitz for animal care. This work was supported by the Deutsche Forschungsgemeinschaft (DFG) through GK592 to SB, AB, LN and THW, FOR832 to LN and THW and through DFG Yu47/2-1 to PY.

Author contributions: SB wrote the paper and performed experiments; DD, TS, FW, EH, SP, HW, AB and AS performed experiments; PY and GCM provided Ali5 mice; LN contributed to Ca-signalling experiments, BAFF-R experiments and discussions; THW wrote the paper, performed experiments and supervised the experiments.

Conflict of interest

The authors declare that they have no conflict of interest.

References

Allman D, Lindsley RC, DeMuth W, Rudd K, Shinton SA, Hardy RR (2001) Resolution of three nonproliferative immature splenic B cell subsets reveals multiple selection points during peripheral B cell maturation. *J Immunol* **167:** 6834–6840

Allman D, Pillai S (2008) Peripheral B cell subsets. *Curr Opin Immunol* **20:** 149–157

Alugupalli KR, Leong JM, Woodland RT, Muramatsu M, Honjo T, Gerstein RM (2004) B1b lymphocytes confer T cell-independent long-lasting immunity. *Immunity* **21:** 379–390

Berland R, Wortis HH (2002) Origins and functions of B-1 cells with notes on the role of CD5. *Annu Rev Immunol* **20:** 253–300

Cancro MP (2009) Signalling crosstalk in B cells: managing worth and need. *Nat Rev Immunol* **9:** 657–661

Casola S, Otipoby KL, Alimzhanov M, Humme S, Uyttersprot N, Kutok JL, Carroll MC, Rajewsky K (2004) B cell receptor signal strength determines B cell fate. *Nat Immunol* **5:** 317–327

Derudder E, Cadera EJ, Vahl JC, Wang J, Fox CJ, Zha S, Van Loo G, Pasparakis M, Schlissel MS, Schmidt-Supprian M, Rajewsky K (2009) Development of immunoglobulin lambda-chain-positive B cells, but not editing of immunoglobulin kappa-chain, depends on NF-kappaB signals. *Nat Immunol* **10:** 647–654

Dorshkind K, Montecino-Rodriguez E (2007) Fetal B-cell lymphopoiesis and the emergence of B-1-cell potential. *Nat Rev Immunol* **7:** 213–219

Gay D, Saunders T, Camper S, Weigert M (1993) Receptor editing: an approach by autoreactive B cells to escape tolerance. *J Exp Med* **177:** 999–1008

Haas KM, Poe JC, Steeber DA, Tedder TF (2005) B-1a and B-1b cells exhibit distinct developmental requirements and have unique functional roles in innate and adaptive immunity to S. pneumoniae. *Immunity* **23:** 7–18

Hao Z, Rajewsky K (2001) Homeostasis of peripheral B cells in the absence of B cell influx from the bone marrow. *J Exp Med* **194:** 1151–1164

Hardy RR, Kincade PW, Dorshkind K (2007) The protean nature of cells in the B lymphocyte lineage. *Immunity* **26:** 703–714

Harfst E, Andersson J, Grawunder U, Ceredig R, Rolink AG (2005) Homeostatic and functional analysis of mature B cells in lambda5-deficient mice. *Immunol Lett* **101:** 173–184

Hashimoto A, Takeda K, Inaba M, Sekimata M, Kaisho T, Ikehara S, Homma Y, Akira S, Kurosaki T (2000) Cutting edge: essential role of phospholipase C-gamma 2 in B cell development and function. *J Immunol* **165:** 1738–1742

Hebeis BJ, Klenovsek K, Rohwer P, Ritter U, Schneider A, Mach M, Winkler TH (2004) Activation of virus-specific memory B cells in the absence of T cell help. *J Exp Med* **199:** 593–602

Herzog S, Reth M, Jumaa H (2009) Regulation of B-cell proliferation and differentiation by pre-B-cell receptor signalling. *Nat Rev Immunol* **9:** 195–205

Hess J, Werner A, Wirth T, Melchers F, Jack HM, Winkler TH (2001) Induction of pre-B cell proliferation after *de novo* synthesis of the pre-B cell receptor. *Proc Natl Acad Sci USA* **98:** 1745–1750

Hoffmann A, Kerr S, Jellusova J, Zhang J, Weisel F, Wellmann U, Winkler TH, Kneitz B, Crocker PR, Nitschke L (2007) Siglec-G is a B1 cell-inhibitory receptor that controls expansion and calcium signaling of the B1 cell population. *Nat Immunol* **8:** 695–704

Iwakoshi NN, Lee AH, Vallabhajosyula P, Otipoby KL, Rajewsky K, Glimcher LH (2003) Plasma cell differentiation and the unfolded protein response intersect at the transcription factor XBP-1. *Nat Immunol* **4:** 321–329

Kantor AB, Herzenberg LA (1993) Origin of murine B cell lineages. *Annu Rev Immunol* **11:** 501–538

Kraus M, Alimzhanov MB, Rajewsky N, Rajewsky K (2004) Survival of resting mature B lymphocytes depends on BCR signaling via the Igalpha/beta heterodimer. *Cell* **117:** 787–800

Kulathu Y, Grothe G, Reth M (2009) Autoinhibition and adapter function of Syk. *Immunol Rev* **232:** 286–299

Lam KP, Rajewsky K (1999) B cell antigen receptor specificity and surface density together determine B-1 versus B-2 cell development. *J Exp Med* **190:** 471–477

Lennon GG, Perry RP (1985) C mu-containing transcripts initiate heterogeneously within the IgH enhancer region and contain a novel 5′-nontranslatable exon. *Nature* **318:** 475–478

Mackay F, Schneider P (2009) Cracking the BAFF code. *Nat Rev Immunol* **9:** 491–502

Martin F, Kearney JF (2001) B1 cells: similarities and differences with other B cell subsets. *Curr Opin Immunol* **13:** 195–201

Martin F, Kearney JF (2002) Marginal-zone B cells. *Nat Rev Immunol* **2:** 323–335

Martin F, Oliver AM, Kearney JF (2001) Marginal zone and B1 B cells unite in the early response against T-independent blood-borne particulate antigens. *Immunity* **14:** 617–629

Martincic K, Alkan SA, Cheatle A, Borghesi L, Milcarek C (2009) Transcription elongation factor ELL2 directs immunoglobulin secretion in plasma cells by stimulating altered RNA processing. *Nat Immunol* **10:** 1102–1109

Melchers F (2005) The pre-B-cell receptor: selector of fitting immunoglobulin heavy chains for the B-cell repertoire. *Nat Rev Immunol* **5:** 578–584

Montecino-Rodriguez E, Leathers H, Dorshkind K (2006) Identification of a B-1 B cell-specified progenitor. *Nat Immunol* **7:** 293–301

Nemazee D, Hogquist KA (2003) Antigen receptor selection by editing or downregulation of V(D)J recombination. *Curr Opin Immunol* **15:** 182–189

Niiro H, Clark EA (2002) Regulation of B-cell fate by antigen-receptor signals. *Nat Rev Immunol* **2:** 945–956

O'Gorman S, Dagenais NA, Qian M, Marchuk Y (1997) Protamine-Cre recombinase transgenes efficiently recombine target sequences in the male germ line of mice, but not in embryonic stem cells. *Proc Natl Acad Sci USA* **94:** 14602–14607

Patke A, Mecklenbrauker I, Erdjument-Bromage H, Tempst P, Tarakhovsky A (2006) BAFF controls B cell metabolic fitness through a PKC—and Akt-dependent mechanism. *J Exp Med* **203:** 2551–2562

Pillai S, Cariappa A, Moran ST (2004) Positive selection and lineage commitment during peripheral B-lymphocyte development. *Immunol Rev* **197:** 206–218

Pillai S, Cariappa A, Moran ST (2005) Marginal zone B cells. *Annu Rev Immunol* **23:** 161–196

Radic MZ, Erikson J, Litwin S, Weigert M (1993) B lymphocytes may escape tolerance by revising their antigen receptors. *J Exp Med* **177:** 1165–1173

Smith SH, Cancro MP (2003) Cutting edge: B cell receptor signals regulate BLyS receptor levels in mature B cells and their immediate progenitors. *J Immunol* **170:** 5820–5823

Tiegs SL, Russell DM, Nemazee D (1993) Receptor editing in self-reactive bone marrow B cells. *J Exp Med* **177:** 1009–1020

Tze LE, Schram BR, Lam K-P, Hogquist KA, Hippen KL, Liu J, Shinton SA, Otipoby KL, Rodine PR, Vegoe AL, Kraus M, Hardy RR, Schlissel MS, Rajewsky K, Behrens TW (2005) Basal immunoglobulin signaling actively maintains developmental stage in immature B cells. *PLoS Biol* **3:** e82

Vettermann C, Herrmann K, Jäck H-M (2006) Powered by pairing: the surrogate light chain amplifies immunoglobulin heavy chain signaling and pre-selects the antibody repertoire. *Semin Immunol* **18:** 44–55

Wang D, Feng J, Wen R, Marine JC, Sangster MY, Parganas E, Hoffmeyer A, Jackson CW, Cleveland JL, Murray PJ, Ihle JN (2000) Phospholipase Cgamma2 is essential in the functions of B cell and several Fc receptors. *Immunity* **13:** 25–35

Watanabe N, Nisitani S, Ikuta K, Suzuki M, Chiba T, Honjo T (1999) Expression levels of B cell surface immunoglobulin regulate efficiency of allelic exclusion and size of autoreactive B-1 cell compartment. *J Exp Med* **190:** 461–469

Yu P, Constien R, Dear N, Katan M, Hanke P, Bunney TD, Kunder S, Quintanilla-Martinez L, Huffstadt U, Schroder A, Jones NP, Peters T, Fuchs H, de Angelis MH, Nehls M, Grosse J, Wabnitz P, Meyer TP, Yasuda K, Schiemann M *et al* (2005) Autoimmunity and inflammation due to a gain-of-function mutation in phospholipase C gamma 2 that specifically increases external Ca2 + entry. *Immunity* **22:** 451–465

